Journal of Computational and Applied Mathematics 236 (2011) 801–811

Contents lists available at SciVerse ScienceDirect

Journal of Computational and Applied Mathematics

journal homepage: www.elsevier.com/locate/cam

Mesh-dependent stability for finite element approximations of parabolic equations with mass lumping

Liyong Zhu [a,*], Qiang Du [b]

[a] LMIB and School of Mathematics and System Science, Beihang University, 100191, Beijing, PR China

[b] Department of Mathematics, Pennsylvania State University, University Park, PA 16802, USA

ARTICLE INFO

Keywords:
Stable time step size
Finite element method
Unstructured mesh
Parabolic equation
Mass lumping

ABSTRACT

In this paper, based on some mesh-dependent estimates on the extreme eigenvalues of a general finite element system defined on a simplicial mesh, novel and sharp bounds on the permissible time step size are derived for the mass lumping finite element approximations of parabolic equations. The bounds are dependent not only on the mesh size but also on the mesh shape. These results provide guidance to the stability of numerical solutions of parabolic problems in relation to the unstructured geometric meshing. Numerical experiments on both uniform meshes and adaptive meshes are presented to validate the theoretical analysis.

© 2011 Elsevier B.V. All rights reserved.

1. Introduction

We consider the numerical solution of some parabolic equations based on a spatial finite element discretization and a time marching scheme. Such a process often involves the spatial mesh generation and optimization, the assembly of finite element systems using the finite element basis, and the iterations and marching in the temporal direction. For spatial discretizations, finite element methods on unstructured simplicial meshes (including, in particular, two-dimensional triangular meshes and three-dimensional tetrahedral meshes) have become very popular, and the coupling with explicit time marching remains a dominant engineering practice. Yet, it is known that explicit time marching is only numerically stable under suitable time step constraints. Thus, deriving a sharp permissible bound on the time step size can be useful for the efficient implementation of explicit marching schemes.

As a continuation of the series of works presented in [1,2], the goal of our study undertaken here is to explore the relations among the mesh geometry and the stable time step size for a mass-lumped explicit Euler-type time integration scheme for parabolic problems. Although there have been earlier studies on the relationship between the mesh geometry and the stable time step size for explicit time integration schemes for dynamic problems in the finite element literature [3,4], few precise and explicit descriptions of such a relation for general finite element spaces are available. Recently in [2], a precise relation is established between the mesh geometry and the spectral condition number of stiffness matrix for some typical second-order elliptic equations discretized by general finite element methods based on unstructured simplicial meshes in any space dimension, which shed new light into the study of the precise relationship between mesh geometry and the spectral properties of the algebraic systems associated with finite element approximations of elliptic operators. The framework outlined in [2] may also be applicable to other problems including time-dependent problems.

In this work, based on an earlier framework on the estimates of stiffness matrix eigenvalues given in [5,6] and the derivation of an explicit trace formula for the element stiffness matrix corresponding to the finite element approximation to the elliptic operator in [2], we derive some new bounds on stable time step sizes for explicit time integration schemes

* Corresponding author.
E-mail addresses: liyongzhu@buaa.edu.cn (L. Zhu), qdu@math.psu.edu (Q. Du).

0377-0427/$ – see front matter © 2011 Elsevier B.V. All rights reserved.
doi:10.1016/j.cam.2011.05.030

with a general mass-lumped finite element discretization for some model parabolic equations. These bounds are sharp and explicitly expressed by some universal mesh geometric quantities which are dependent not only on mesh size but also on mesh shape. The obtained results are very helpful for us to understand deeply the relationship between the stability and the mesh geometry for general high-order mass-lumped finite element methods which have important applications in many problems [7–9]. We also perform some numerical experiments to verify the theoretical results.

This paper is organized as follows. In Section 2, we recall the basic finite element spatial discretization of a parabolic equation and describe the main issues that we are concerned with. Then, in Section 3, some existing results on extreme eigenvalue estimates for general finite element spaces are briefly stated and a new estimate of the largest eigenvalue of the matrix $M^{-1}K$ is derived. In Section 4, we derive the mesh-dependent time step size conditions for the stability of explicit time integration schemes. In Section 5, numerical examples are provided to substantiate the theoretical analysis. A final conclusion is given in Section 6.

2. The finite element spatial discretization of a parabolic equation

Given an open bounded convex domain $\Omega \in \mathbb{R}^d$ with a Lipschitz-continuous boundary and a finite time interval $(0, T]$, consider the following time-dependent parabolic equation

$$\begin{cases} \dfrac{\partial u(\mathbf{x}, t)}{\partial t} = \displaystyle\sum_{i,j=1}^{d} \frac{\partial}{\partial x_i}\left(a_{ij}\frac{\partial u}{\partial x_j}\right) + f(\mathbf{x}, t), & \text{in } \Omega \times (0, T], \\ u(\mathbf{x}, 0) = u_0(\mathbf{x}), & \text{in } \Omega, \\ u(\mathbf{x}, t) = 0, & \text{on } \partial\Omega \times (0, T], \end{cases} \tag{1}$$

where the coefficient matrix $\tilde{A} = (a_{ij})_{i,j=1}^{d}$ is assumed to be constant in time, and furthermore, $\tilde{A}$ is assumed to be symmetric positive definite, smooth and uniformly bounded in $\bar{\Omega}$ while $f \in C^1(0, T; L^2(\Omega))$. The independence of time simplifies the notation, though much of our discussion remains valid for time-dependent coefficients. We also choose to work with the homogeneous Dirichlet boundary condition for simplicity.

The finite element method is employed to discretize in the spatial dimensions. Let $\mathcal{T}$ denote the finite element mesh (a triangulation, or equivalently, a simplicial mesh, for much of our discussion). An appropriate finite element space, $V_h \subset H_0^1(\Omega)$, with suitably chosen nodal basis functions $\{\phi_j\}_{j=1}^{N}$ may then be employed to discretize the above continuous problem, resulting in the finite element approximations as follows,

$$\int_\Omega \frac{\partial u_h(\mathbf{x}, t)}{\partial t} v_h \, \mathrm{d}\mathbf{x} + a_\Omega(u_h, v_h) = \int_\Omega f v_h \, \mathrm{d}\mathbf{x}, \quad \forall\, v_h \in V_h, \tag{2}$$

and the bilinear form $a_\Omega = a_\Omega(u, v)$ is given by

$$a_\Omega(u, v) := \int_\Omega \sum_{i,j=1}^{d} \left(a_{ij}\frac{\partial u}{\partial x_i}\frac{\partial v}{\partial x_j}\right) \mathrm{d}\mathbf{x} \tag{3}$$

for any $u, v \in H_0^1(\Omega)$. Details on the properties of V_h are to be stated later. Let $\{\phi_j\}_1^N$ be the finite element nodal basis of V_h and then for any $u_h \in V_h$, we denote by $\{\mathbf{u}_i\}$ the vector containing the coordinates of u_h^i with respect to the basis $\{\phi_j\}$, so that $u_h^i = \sum(\mathbf{u}_i)_j\phi_j$.

In order to solve the above system of ordinary differential equations, we further consider the most popular explicit forward Euler first-order time integration scheme which can be written as

$$\int_\Omega \frac{u_h^{i+1} - u_h^i}{\Delta t} v_h \, \mathrm{d}\mathbf{x} + a_\Omega(u_h^i, v_h) = \int_\Omega f^i v_h \, \mathrm{d}\mathbf{x}, \quad \forall v_h \in V_h, \tag{4}$$

where Δt is the time step size, and u_h^i is the approximation solution of $u(\mathbf{x}, t)$ at time $i\Delta t$ and $f^i = f(\mathbf{x}, i\Delta t)$. In matrix notation, the approximation solution $\mathbf{u}_{i+1}$ satisfies

$$\tilde{M}\mathbf{u}_{i+1} = (\tilde{M} - \Delta t K)\mathbf{u}_i + \Delta t\mathbf{f}_i, \quad i = 1, 2, 3, \ldots, \tag{5}$$

where $(\mathbf{f}_i)_j = \int_\Omega f^i\phi_j \mathrm{d}\mathbf{x}$, K and $\tilde{M}$ are respectively the $N \times N$ stiffness and mass matrices, respectively, generated by the finite element basis $\{\phi_i\}$, that is,

$$K = (k_{ij}), \quad k_{ij} = a_\Omega(\phi_i, \phi_j) \quad \text{and} \quad \tilde{M} = (m_{ij}), \quad m_{ij} = \int_\Omega \phi_i\phi_j \, \mathrm{d}\mathbf{x}. \tag{6}$$

We note that for variable and time-dependent coefficient problems, the only complication is that K depends on the number of time steps. Since our discussions focus mostly on the properties of (4) at a single step, they can be easily adapted to treat variable coefficients as well.

The explicit forward difference scheme (5) is widely employed in practice, and often $\tilde{M}$ is changed into a diagonal by an approximation technique or numerical quadrature that is called *mass lumping*, so that its inverse can be obtained readily. The mass lumping is to substitute the mass matrix $\tilde{M}$ with a diagonal matrix $M = \mathrm{diag}(M_1, M_2, \ldots, M_N)$ with

$$M_i = \sum_{j=1}^{N} m_{ij}, \quad i = 1, 2, \ldots, N. \tag{7}$$

Thus, we can get the solution at the $(i+1)$th step by

$$\mathbf{u}_{i+1} = (I - \Delta t M^{-1} K)\mathbf{u}_i + \Delta t M^{-1}\mathbf{f}_i, \quad i = 1, 2, 3, \ldots, N. \tag{8}$$

However, the time step size Δt must be constrained in order to satisfy the stability condition associated with the explicit scheme. Obviously, to derive a sharp permissible time step size constraint can be helpful for the efficient implementation of explicit schemes.

In our work here, we focus on getting sharp estimates, in terms of their dependence on the mesh geometry, for the time-stability constraints of the explicit scheme. These issues are intimately connected to the spectral properties of the matrices $(I - \Delta t M^{-1} K)$ or equivalently $(I - \Delta t M^{-1/2} K M^{-1/2})$. Indeed, since M is symmetric and positive definite, we have

$$\Lambda(M^{-1}K) = \Lambda(M^{1/2}M^{-1}KM^{-1/2}) = \Lambda(M^{-1/2}KM^{-1/2}), \tag{9}$$

where $\Lambda(A)$ express the set of eigenvalues of A. Hence, the analysis should essentially rely on the spectral properties of $M^{-1/2}KM^{-1/2}$. The latter is naturally related to the analysis of the spectral properties of the finite element discretizations of the corresponding elliptic equations which has been carefully carried out in [2].

3. Some results on extreme eigenvalue estimates

In this section, we recall briefly the abstract framework on extreme eigenvalues estimate of the global finite element stiffness (mass) matrix for general symmetric second-order elliptic equations given in [6] and the extreme eigenvalue estimates on element stiffness (mass) matrix given in [2] for a general finite element discretization. Then, we derive some novel estimates on the largest eigenvalue of the matrix $M^{-1}K$. These results form the basis for further discussions on the mesh-dependent stability.

3.1. An abstract framework on extreme eigenvalue estimates

To study (1), we first consider the corresponding second-order elliptic boundary value problem,

$$\begin{cases} -\sum_{i,j=1}^{d} \dfrac{\partial}{\partial x_i}\left(a_{ij}\dfrac{\partial u}{\partial x_j}\right) = f, & \text{in } \Omega, \\ u = 0, & \text{on } \partial\Omega, \end{cases} \tag{10}$$

with $f \in L^2(\Omega)$. The corresponding variational weak form is as follows [10]: find $u \in H_0^1(\Omega)$, such that

$$a_\Omega(u, v) = \int_\Omega f v \, \mathrm{d}\mathbf{x}, \quad \forall v \in H_0^1(\Omega). \tag{11}$$

Obviously, the stiffness matrix K defined by (6), is both symmetric and positive definite. Denote the element matrices corresponding to K by K_τ for any (simplicial) element $\tau \in \mathcal{T}$. We use n to denote the dimension of K_τ, which corresponds to the degree of freedoms or the number of nodal basis functions for the element τ.

The eigenvalues of K are denoted by $\{\lambda_i^K\}_{i=1}^N$ which are ordered by

$$\lambda_1^K \le \lambda_2^K \le \cdots \le \lambda_N^K.$$

In this notation, λ_1^K is the minimal eigenvalue of K, and λ_N^K are the maximal eigenvalues. Similarly, we use $\{\lambda_i^{K_\tau}\}_{i=1}^n$ to denote the eigenvalue of K_τ which are also ordered by

$$\lambda_1^{K_\tau} \le \lambda_2^{K_\tau} \le \cdots \le \lambda_n^{K_\tau}.$$

In [5,6], some general estimates on the extreme eigenvalues of the global stiffness matrix in relation to that of the element stiffness matrix were given as follows:

$$\max_{\tau\in\mathcal{T}}(\lambda_n^{K_\tau}) \le \lambda_N^K \le D_* \max_{\tau\in\mathcal{T}}(\lambda_n^{K_\tau}), \tag{12}$$

where D_* is the maximal number of elements meeting at a nodal point, in this paper, we always consider those meshes with uniformly bounded D_*.

3.2. Extreme eigenvalue estimates of the element stiffness matrix

To bound the extreme eigenvalues of global stiffness matrices, by (12), we need estimates on $\lambda_n^{K_\tau}$ for the element stiffness matrices. In this subsection, we state the extreme eigenvalue estimates of element stiffness matrix given in [2]. First, we state some assumptions on the finite element spaces under consideration.

Assumptions on the finite element space and nodal basis: on a reference simplex described by

$$\tau_0 = \left\{(b_1, b_2, \ldots, b_{d+1}) \mid b_i \geq 0, \sum b_j = 1\right\},$$

the nodal basis on τ_0 is assumed to involve a linear combination of the partial products of $\{b_j\}$ only. For any (simplicial) element $\tau \in \mathcal{T}$, $\{L_i(\{b_j\})\}_{i=1}^n$ is used to denote a general form of the nodal basis which, when restricted to τ, is given by the same nodal basis defined on τ_0 with $(b_1, b_2, \ldots, b_{d+1})$ being the corresponding barycentric coordinates of τ. And the finite element approximation is given by functions whose restrictions on τ are linear combinations of $\{L_i\}$. Concerning the finite element space, an additional assumption is made that the nodal basis on τ_0 is invariant with respect to the permutation of the vertices, a property that is satisfied by most of the finite element spaces.

Let us introduce the notation $\mathcal{Q}_d(\tau)$ and γ_n^d as follows:

$$\mathcal{Q}_d(\tau) = \frac{1}{|\tau|}\sum_{i=1}^{d+1}|A_i|^2, \tag{13}$$

for any d-dimensional simplex τ with $|\tau|$ being its volume and $\{A_i\}_{i=1}^{d+1}$ being the areas (volumes) of its $(d-1)$-dimensional faces;

$$\gamma_n^d = \frac{1}{d^3(d+1)|\tau_0|}\sum_{m=1}^{n}\sum_{j=1}^{d+1}\sum_{k=1}^{d+1}\int_{\tau_0}\left(\frac{\partial L_m}{\partial b_j} - \frac{\partial L_m}{\partial b_k}\right)^2 \mathrm{d}\mathbf{x}, \tag{14}$$

where τ_0 is the standard reference simplex defined as above. For the general diffusion problem (10), we further assume that

$$0 < \beta_1^\tau I \leq \tilde{A}^\tau(\mathbf{x}) \leq \beta_2^\tau I \tag{15}$$

uniformly for $\mathbf{x} \in \tau$ for some positive constants β_1^τ and β_2^τ, where $\tilde{A}^\tau(\mathbf{x})$ is the restriction of the coefficient matrix $\tilde{A}$ on τ, and $\mathbf{I}$ is the unit matrix. Here we state the estimates for the largest eigenvalue of the element stiffness matrix K_τ given in [2] as follows.

Lemma 3.1. *For any general finite element spaces defined on a simplicial mesh τ with the nodal basis on any d-dimensional simplex $\tau \in \mathcal{T}$ satisfying the invariance property specified above, the largest eigenvalue of the element matrix K_τ corresponding to the Eq. (10) has the estimates:*

$$\frac{\beta_1^\tau \gamma_n^d}{n-1}\mathcal{Q}_d(\tau) \leq \lambda_n^{K_\tau} \leq \beta_2^\tau \gamma_n^d \mathcal{Q}_d(\tau) \tag{16}$$

where n is the cardinality of the set of local nodal basis functions, γ_n^d is the positive constant defined by (14), $\mathcal{Q}_d(\tau)$ is as defined by (13).

As in [2], it is important to note that γ_n^d is a positive constant that depends only on the corresponding basis functions on the reference simplex τ_0 and is independent of the geometry of the particular element τ while the other factor $\mathcal{Q}_d(\tau)$ is completely independent of the choice of the finite element spaces (as long as they take some invariant basis).

The above estimate does provide a precise control on the contribution due to the mesh geometry on the largest eigenvalue of the element stiffness matrix associated with the elliptic operator which is crucial for estimating the stable time step size for a parabolic equation.

3.3. A lemma on element mass matrix

In order to estimate the permissible time step size, the dependence of the extreme eigenvalues of the element mass matrices on the mesh geometry is needed. The computation about this dependence is rather simple. Denote the entries of global mass matrix corresponding to the element τ by the diagonal matrix $M_\tau = \mathrm{diag}(M_{N_1}, M_{N_2}, \ldots, M_{N_n})$ where $N_1, N_2, \ldots, N_n$ are the indices of the nodes on the element τ. We use M_{τ_0} to denote the element mass matrix on the reference element τ_0 defined by

$$M_{\tau_0} = (m_{ij}^{\tau_0}), \quad m_{ij}^{\tau_0} = \int_{\tau_0}\phi_i\phi_j\,\mathrm{d}\mathbf{x}.$$

Then, simple calculations give the following lemma.

Lemma 3.2. *For the lumped mass matrix defined by (7), the corresponding element mass matrix M_τ satisfies:*

$$M_\tau = S_\tau\frac{M_{\tau_0}}{|\tau_0|}, \tag{17}$$

where $S_\tau = \mathrm{diag}(S_{N_1}, S_{N_2}, \ldots, S_{N_n})$ *and* S_{N_i} *is the lumped areas with index* N_i *(summation of areas (volumes) of elements that share the node* N_i*). Consequently,*

$$\min_{\tau\in\mathcal{T}} \lambda_1^{M_\tau} = \delta_n \min_i S_i, \qquad \max_{\tau\in\mathcal{T}} \lambda_n^{M_\tau} = \sigma_n \max_i S_i, \tag{18}$$

where δ_n *and* σ_n *are two constants given by*

$$\delta_n = \frac{1}{|\tau_0|}\lambda_1^{M_{\tau_0}}, \qquad \sigma_n = \frac{1}{|\tau_0|}\lambda_n^{M_{\tau_0}}. \tag{19}$$

Note that the constants δ_n and σ_n are independent of the element τ but rely on t_0 and the corresponding local finite element basis.

3.4. A new estimate on the largest eigenvalue of $M^{-1}K$

In this subsection, we estimate the largest eigenvalue of $M^{-1}K$, or equivalently $M^{-1/2}KM^{-1/2}$, where $M^{-1/2}$ is the diagonal matrix whose diagonal entries are $M_i^{-1/2}$. This is the basis for our study given here.

Denote

$$J_\tau = M_\tau^{-\frac{1}{2}} K_\tau M_\tau^{-\frac{1}{2}}.$$

Since the matrix $M^{-1/2}KM^{-1/2}$ can be assembled from the matrices $\{J_\tau\}$ in the same way as the global stiffness matrix K is assembled from the element stiffness matrices K_τ, with (9) and (12), we have

$$\max_\tau \lambda_{\max}(J_\tau) \le \lambda_{\max}(M^{-1}K) \le D_* \max_\tau \lambda_{\max}(J_\tau). \tag{20}$$

Then the key is to estimate the bound of the eigenvalues of J_τ.

Let $P = M_\tau^{-1/2}$ for simplicity. Obviously, P is a symmetric and positive definite matrix with $P' = P$ where $'$ denotes the matrix transpose. Using the properties of the Rayleigh quotient on a matrix, we have

$$\begin{aligned}
\lambda_{\max}(PK_\tau P) &= \lambda_{\max}(P'K_\tau P) = \max_{X\in\mathbb{R}^n, X\neq\mathbf{0}} \left\{ \frac{X'(P'K_\tau P)X}{X'X} \right\} \\
&= \max_{X\in\mathbb{R}^n, X\neq\mathbf{0}} \left\{ \frac{(PX)'K_\tau(PX)}{(PX)'(PX)} \frac{X'P'PX}{X'X} \right\} \\
&\le \lambda_{\max}(K_\tau)\lambda_{\max}(P'P) = \lambda_{\max}(K_\tau)\lambda_{\min}^{-1}(M_\tau).
\end{aligned} \tag{21}$$

On the other hand, by taking the special vector $X = \hat{X}$ such that $P\hat{X}$ is an eigenvector corresponding to the largest eigenvalue of the matrix K_τ, we obtain

$$\begin{aligned}
\lambda_{\max}(PK_\tau P) &= \lambda_{\max}(P'K_\tau P) = \max_{X\in\mathbb{R}^n, X\neq\mathbf{0}} \left\{ \frac{X'(P'K_\tau P)X}{X'X} \right\} \\
&= \max_{X\in\mathbb{R}^n, X\neq\mathbf{0}} \left\{ \frac{(PX)'K_\tau(PX)}{(PX)'(PX)} \frac{X'P'PX}{X'X} \right\} \\
&\ge \frac{(P\hat{X})'K_\tau(P\hat{X})}{(P\hat{X})'(P\hat{X})} \frac{\hat{X}'P'P\hat{X}}{\hat{X}'\hat{X}} \\
&\ge \lambda_{\max}(K_\tau)\lambda_{\min}(M_\tau^{-1}) = \lambda_{\max}(K_\tau)\lambda_{\max}^{-1}(M_\tau).
\end{aligned} \tag{22}$$

Then, by (18), (21) and (22), we have the following estimates for the largest eigenvalue of the element matrix $M_\tau^{-1/2}K_\tau M_\tau^{-1/2}$.

Lemma 3.3. *For any general finite element spaces defined on a simplicial mesh* $\mathcal{T}$ *with the nodal basis on any d-dimensional simplex* $\tau \in \mathcal{T}$ *satisfying the invariance property specified above, the largest eigenvalue of the element matrix* $M_\tau^{-1/2}K_\tau M_\tau^{-1/2}$ *has the estimates:*

$$\frac{|\tau_0|\lambda_n^{K_\tau}}{S_{\max}^\tau \lambda_n^{M_{\tau_0}}} \le \lambda_{\max}(M_\tau^{-1/2}K_\tau M_\tau^{-1/2}) \le \frac{|\tau_0|\lambda_n^{K_\tau}}{S_{\min}^\tau \lambda_1^{M_{\tau_0}}} \tag{23}$$

where n *is the cardinality of the set of local nodal basis functions,* $S_{\max}^\tau = \max_{v_i\in\tau} S_{v_i}$ *and* $S_{\min}^\tau = \min_{v_i\in\tau} S_{v_i}$.

With (20), (16) and (23), we can get the following estimates on the largest eigenvalue of $M^{-1}K$.

Theorem 3.1. *Under the assumptions on the finite element spaces made earlier, the largest eigenvalue of the matrix $M^{-1}K$ has the estimates:*

$$\hat{\gamma}_n^d \max_{\tau\in\mathcal{T}} \frac{\beta_1^\tau \mathcal{Q}_d(\tau)}{S_{\max}^\tau} \le \lambda_{\max}(M^{-1}K) \le D_* \tilde{\gamma}_n^d \max_{\tau\in\mathcal{T}} \frac{\beta_2^\tau \mathcal{Q}_d(\tau)}{S_{\min}^\tau}, \tag{24}$$

where n is the cardinality of the set of local nodal basis functions, $\hat{\gamma}_n^d$ and $\tilde{\gamma}_n^d$ are defined by

$$\hat{\gamma}_n^d = \frac{\lambda_{\max}^{-1}(M_{\tau_0})}{(n-1)}|\tau_0|\gamma_n^d, \qquad \tilde{\gamma}_n^d = \lambda_{\min}^{-1}(M_{\tau_0})|\tau_0|\gamma_n^d \tag{25}$$

and D∗ is the maximum number of elements meeting at a single vertex.

Remark 3.1. Here we point out that the constants $\hat{\gamma}_n^d$ and $\tilde{\gamma}_n^d$ are independent of the specified element τ but only on t_0 as well as the corresponding local finite element basis, while the other factors in the bounds, which are dependent of mesh geometry and equations, are completely independent of the choice of the finite element spaces.

Remark 3.2. For the general case (with no mass lumping), similar estimates are derived in [11]. Since the matrix $M^{-1/2}KM^{-1/2}$ is not assembled from the element matrix $M_\tau^{-1/2}K_\tau M_\tau^{-1/2}$ directly as that in the mass lumping case, a "gradual volume change condition" is required in order to derive the desired estimates [11]. For the mass lumping case considered here, if the mesh also satisfies the "gradual volume change condition" as imposed in [11], then there exist two positive constants c_1 and c_2 satisfying

$$c_1|\tau| \le S_{\min}^\tau \le S_{\max}^\tau \le c_2|\tau|.$$

Thus, we get consistent results (in terms of the same mesh geometry quantity) between the two cases.

4. Mesh-dependent stability condition for the explicit time integration

In this section, we apply the general estimates in the previous sections to derive the mesh-dependent permissible time step sizes for the explicit time integration scheme for some model parabolic equations. Some of these estimates are widely known and are consistent with the popular understanding in the finite element and meshing community, while others are new and are interesting on their own.

4.1. Stability condition for the explicit scheme

Let $\mathbf{u}_i^*$ be the numerical solution which satisfies

$$M\mathbf{u}_{i+1}^* = (M - \Delta t K)\mathbf{u}_i^* + \Delta t \mathbf{f}_i, \quad i = 1, 2, 3, \ldots. \tag{26}$$

Let $\mathbf{e}_i = \mathbf{u}_i^* - \mathbf{u}_i$. Then, by multiplying M^{-1} on the two hands of (26) and subtracting (26) from (8), one can obtain the recurrence on error

$$\mathbf{e}_{i+1} = (I - \Delta t M^{-1}K)\mathbf{e}_i. \tag{27}$$

The following norms are usually used to analyze the stability,

$$\|\mathbf{e}_i\|_{L^2(\Omega)}^2 = (\mathbf{e}_i' M \mathbf{e}_i); \qquad \|\mathbf{e}_i\|_{H^1(\Omega)}^2 = (\mathbf{e}_i' K \mathbf{e}_i). \tag{28}$$

Note that M is both symmetric and positive definite, and, by (27), simple calculation gives

$$\|\mathbf{e}_j\|_{L^2(\Omega)} \le (\lambda_{\max}(I - \Delta t M^{-1}K))^{(j-i)} \|\mathbf{e}_i\|_{L^2(\Omega)}. \tag{29}$$

Similarly, we can get

$$\|\mathbf{e}_j\|_{H^1(\Omega)} \le (\lambda_{\max}(I - \Delta t M^{-1}K))^{(j-i)} \|\mathbf{e}_i\|_{H^1(\Omega)}. \tag{30}$$

Inequalities (29) and (30) indicate how the L^2 and H^1 errors may depend on the spectrum of $(I - \Delta t M^{-1}K)$. We thus have a stability condition which can be found in a great deal of existing literature (see, e.g., [3]).

Lemma 4.1. *The explicit differencing (4) is stable with respect to L^2 norm and H^1 norm if the time step size Δt satisfies*

$$\Delta t < \frac{2}{\lambda_{\max}(M^{-1}K)} = \frac{2}{\lambda_{\max}(M^{-1/2}KM^{-1/2})}. \tag{31}$$

In order to get precise largest permissible time step size estimates, a key point is to give precise and exact estimates on $\lambda_{\max}(M^{-1}K)$ for general finite element spaces which are given in (24). Combining with the stability condition (31), we can get the following exact and precise stable time step size estimates for general finite element spaces defined on a simplicial mesh.

Theorem 4.1. *For any finite element space defined on a simplicial mesh $\mathcal{T}$ with the nodal basis on any d-dimensional simplex $\tau \in \mathcal{T}$ satisfying the assumptions specified above, the stability condition for the time step size Δt is given by*

$$\Delta t < \frac{2}{D_* \tilde{\gamma}_n^d} \min_{\tau \in \mathcal{T}} \frac{S_{\min}^\tau}{\beta_2^\tau \mathcal{Q}_d(\tau)}, \tag{32}$$

where n is the cardinality of the set of local nodal basis functions, $\mathcal{Q}_d(\tau)$ and $\tilde{\gamma}_n^d$ are respectively defined by (13) and (25), and β_2^τ is defined in (15).

We give some remarks on the above stability estimates as follows,

Remark 4.1. In [3], some preliminary discussion on mesh-dependent stable time step size was given for simple linear finite element. Our result is more general as it is applicable to any high-order finite element space. High-order finite element methods with mass lumping are an efficient and effective alternative in many applications [7–9].

Remark 4.2. The estimate of time step size bound (32) implies that the stable time step size of the explicit differencing is mainly a product of two factors, with one being $1/\tilde{\gamma}_n^d$ which is completely independent of the geometry of the particular element τ, and the other being $S_{\min}^\tau/\beta_2^\tau \mathcal{Q}_d(\tau)$, which is completely independent of the choice of the finite element spaces (as long as they take some invariant basis). This can be used to explore the precise relationship between stable time step size and mesh geometry.

4.2. Relating time step size constraint to mesh geometry

We first discuss the effects of the element size on the stable time step size bound when the shape of element remains regular. Consider a simplicial mesh $\mathcal{T}$ with all the simplices $\tau \in \mathcal{T}$ satisfying:

$$\rho_1 |\tau|^{2-2/d} \leq \sum_i A_i^2 \leq \rho_2 |\tau|^{2-2/d}, \quad \forall \tau \in \mathcal{T} \tag{33}$$

for some positive constants ρ_1 and ρ_2, independent of τ. We refer such meshes as being *shape regular*. Meanwhile, we refer a simplicial mesh τ as being *quasi-volume-uniform* if

$$\min_{\tau \in \mathcal{T}} |\tau| \geq \rho_3 \max_{\tau \in \mathcal{T}} |\tau|, \quad \forall \tau \in \mathcal{T} \tag{34}$$

holds for some positive constant ρ_3, independent of τ. Then, we have the following corollary,

Corollary 4.1. *For the explicit time integration scheme (4) discretized by a finite element space with an invariant basis defined on a quasi-volume-uniform (in the sense of (34)) d-dimensional simplicial mesh with h being the mesh parameter (diameter of the largest simplex), if we further assume that all the simplices are shape regular in the sense of (33), then it is stable if the time step size satisfies*

$$\Delta t < c_{(n,d)}^{(1)} h^2 \min_\tau \{1/\beta_2^\tau\}, \tag{35}$$

for some constant $c_{(n,d)}^{(1)}$ which is dependent on the finite element basis on the reference element τ_0 and dimension d, but is independent of h.

Corollary 4.1 follows directly from (13) and (32)–(34). It indicates that, for a uniform mesh with well-shaped elements, the largest permissible time step size Δt for the parabolic equations under consideration is roughly proportional to h^2, where h is the typical edge length of element. Hence, smaller elements require smaller time step sizes and more computation cost. The result in Corollary 4.1 in the linear finite element case with mass *lumping* is widely known in the finite element and meshing community, but not in the case of general finite element spaces.

Now we consider those non-uniform meshes with well-shaped elements and satisfying the shape regular condition (33) but not the quasi-uniform condition (34). This case often happens in adaptive finite element computation. In this case, we have the corollary,

Corollary 4.2. *For the explicit time integration scheme (4) discretized by a finite element space with an invariant basis defined on a shape regular (in the sense of (33)) d-dimensional simplicial mesh, then it is stable if the time step size satisfies*

$$\Delta t < c_{(n,d)}^{(2)} \min_{\tau \in \mathcal{T}} \frac{S_{\min}^\tau}{\beta_2^\tau |\tau|^{1-2/d}} \tag{36}$$

for some constants $c_{(n,d)}^{(2)}$ which are dependent on the finite element basis on the reference element τ_0 and the dimension d, but is independent of mesh geometry.

From the above corollary, for a diffusion equation with isotropic coefficients, we can see that the smallest element usually dictates the size of the time step on a non-uniform mesh with well-shaped elements. The smaller the element size, the smaller the permissible time step sizes, and the longer the time marching takes.

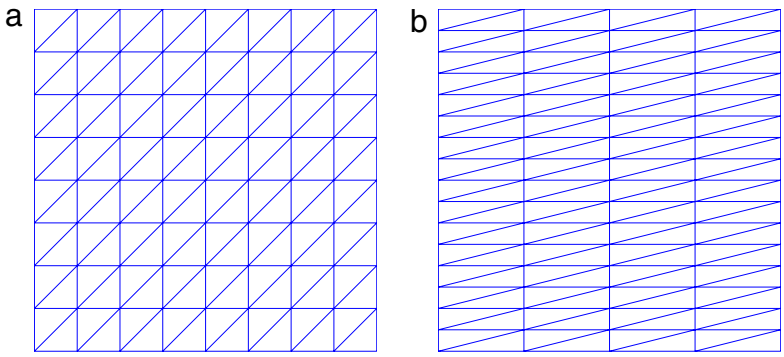


Fig. 1. Uniform triangular meshes with isosceles right triangles (a) and right triangles with small angles (b).

Consider the anisotropic quasi-uniform mesh which satisfies the quasi-uniform condition (34) but not satisfies the regular condition (33). For $\mathcal{Q}_d(\tau)$, the following equivalent relations are given in [2],

$$\mathcal{Q}_2(\tau) = 4\sum_{i=1}^{3}\cot\theta_i^{\tau}, \qquad \mathcal{Q}_3(\tau) = 3\sum_{i=1}^{4}\sum_{j=1,j\neq i}^{4} l_{ij}\cot\theta^{\tau_{ij}}, \tag{37}$$

where θ_i^{τ} is the interior angle against at the edge L_i, and $\theta^{\tau_{ij}}$ is the dihedral angle on the edge L_{ij} with the length l_{ij}. Then, by (32), (34) and (37), we have the following result,

Corollary 4.3. *For the explicit time integration scheme (4) discretized by a finite element space with an invariant basis defined on a quasi-volume-uniform (in the sense of (34)) d-dimensional simplicial mesh, it is stable if the time step size satisfies*

$$\Delta t < c_{(n,2)}^{(3)}|\tau|\min_{\tau\in\mathcal{T}}\left(\beta_2^{\tau}\sum_{i=1}^{3}\cot\theta_i^{\tau}\right)^{-1}, \quad \text{when } d=2; \tag{38}$$

$$\Delta t < c_{(n,3)}^{(4)}|\tau|\min_{\tau\in\mathcal{T}}\left(\beta_2^{\tau}\sum_{i=1}^{4}\sum_{j=1,j\neq i}^{4}\tau_{ij}\cot\theta^{\tau_{ij}}\right)^{-1}, \quad \text{when } d=3; \tag{39}$$

for some constants $c_{(n,2)}^{(3)}$ and $c_{(n,3)}^{(4)}$ which are dependent on the finite element basis on the reference element τ_0 and the dimension d, but are independent of mesh geometry.

The above corollary implies that, for the parabolic equation we consider or parabolic problems with isotropic diffusion coefficients, elements with small angles in two dimension and elements with small dihedral angles in three dimension would force the explicit time integrator to take even smaller time step sizes.

On the non-uniform mesh with irregular element, by (32), the bound on the permissible time step size is decided by both the element shape and the element size, that is the quantity $\min_{\tau\in\mathcal{T}}\{(S_{\min}^{\tau})/(\beta_2^{\tau}Q_d(\tau))\}$.

5. Numerical experiments

In this section, a linear finite element method is implemented. The computational domain is $\Omega = [0,1]\times[0,1]$. Numerical experiments are performed on several sets of meshes, as shown in Figs. 1 and 2, to substantiate the theoretical results obtained in previous sections.

For simplicity, we consider an isotropic heat conduction problem

$$\frac{\partial u}{\partial t} = \frac{\partial^2 u}{\partial x^2} + \frac{\partial^2 u}{\partial y^2} + f,$$

with a homogeneous boundary condition on $\partial\Omega$.

5.1. The uniform mesh cases

In this subsection, the uniform meshes, as shown in Fig. 1, are chosen to examine the effect of mesh geometry on the stability limit in the explicit time integration. We use Δt and Δt_l to denote the stable time step sizes estimated by formulas (31) and (32) respectively. In [11], for the linear element in two-dimensional space, $\tilde{\gamma}_3^2$ are computed as $\tilde{\gamma}_n^d = 6$. For the

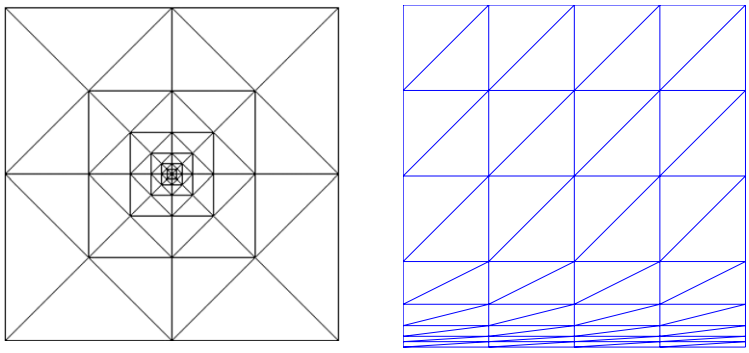


Fig. 2. Adaptive triangular meshes with isosceles right triangles (a) and right triangles with small angles (b).

Table 1
The stability limit on a uniform shape regular mesh.

Mesh	8×8	16×16	32×32	64×64	128×128
Δt	4.0608E−3	9.8604E−4	2.4473E−4	6.1072E−5	1.5261E−5
Δt_l	3.2552E−4	8.1378E−5	2.0344E−5	5.0863E−6	1.2715E−6
CR(Δt)	–	2.04	2.01	2.00	2.00
$\Delta t/\Delta t_l$	12.47	12.12	12.03	12.00	12.00

isosceles right triangle element as shown in Fig. 1(a), denote the isosceles length by a, and then

$$\min_{\tau\in\mathcal{T}} \frac{S^{\tau}_{\min}}{\mathcal{Q}_d(\tau)} = \frac{6|\tau|^2}{\sum_{i=1}^{3} l_i^2} = \frac{6(1/2a^2)^2}{4a^2} = \frac{3a^2}{8}.$$

Here, the parameter $D_* = 6$. Then, by (32), we have

$$\Delta t_l < \frac{2}{6} \times \frac{1}{6} \times \frac{3a^2}{8} = \frac{a^2}{48}. \tag{40}$$

On the right triangle element with a small angle as shown in Fig. 1(b), simple calculation gives

$$\min_{\tau\in\mathcal{T}} \frac{S^{\tau}_{\min}}{\mathcal{Q}_d(\tau)} = \frac{6|\tau|^2}{\sum_{i=1}^{3} l_i^2} = \frac{6s^2}{(8s/\sin(2\theta))} = \frac{3s\sin(2\theta)}{4},$$

where s is the fixed area and θ is the smallest angle in the right triangle [2]. Then, by (32), we have

$$\Delta t_l < \frac{2}{6} \times \frac{1}{6} \times \frac{3s\sin(2\theta)}{4} = (s\sin(2\theta))/24. \tag{41}$$

First, some uniform shape regular meshes with different sizes, as shown in Fig. 1(a), are taken to examine the effect of element size on the stability limit. Here, the $N \times N$ mesh means that the domain is divided uniformly into $N \times N$ squares, with each being divided into two equal triangles. The numerical stability limit Δt, Δt_l and the change ratio $\mathrm{CR}(\Delta t) = \log_2(\Delta t^h/\Delta t^{h/2})$ with respect to Δt, the ratios $\Delta t/\Delta t_l$ for all cases are summarized in Table 1. From Table 1, we see that the change ratio with respect to Δt approximately stays nearly 2, an observation that is consistent with the prediction of the Corollary 4.1. The ratios $\Delta t/\Delta t_l$ also approximate a constant, which implies that the bounds are sharp with respect to the mesh geometry and can characterize well the effect of mesh geometry on the time stability of the marching scheme.

In the second example, a uniform shape irregular mesh with different shape, as shown in Fig. 1(b), is taken to explore the effect of element shape on the stability limit. In this case, the number of all elements are fixed at 64×64, thus the area of element stays fixed. The shape of element is changed with the smallest angle. The numerical stability limit Δt, Δt_l and the ratio $\Delta t/\Delta t_l$ on meshes with different smallest angles are summarized in Table 2. The ratios $\Delta t/\Delta t_l$ are nearly a constant which implies that the bounds are again sharp, up to a constant algebraic factor, in characterizing the effect of mesh geometry on the stability limit. That is, small angle will incur the small stability limit, which is also consistent with the analysis in Corollary 4.3. To be more precise, in Fig. 3 (left), we plot with respect to $\sin(2\theta_{\min})$, the curves of the stability limit. The perfect linear behavior indicates that the stability limit Δt is proportional to $\sin(2\theta_{\min})$.

Table 2
The stability limit on a uniform shape irregular mesh.

Mesh	32×32	16×64	8×128	4×256	2×512
θ	0.250000π	0.077979π	0.019869π	0.004973π	0.001243π
Δt	2.4473E−4	1.1502E−4	3.0408E−5	7.6281E−6	1.9074E−6
Δt_l	2.0344E−5	9.5741E−6	2.5333E−6	6.3560E−7	1.5889E−7
$\Delta t/\Delta t_l$	12.03	12.01	12.00	12.00	12.00

Table 3
The stability limit on a non-uniform shape regular mesh.

Mesh (RF)	8	10	12	14	16
Δt	9.8957E−4	2.4739E−4	6.1848E−5	1.5462E−5	3.8652E−6
Δt_l	4.0690E−5	1.0173E−5	2.5431E−6	6.3578E−7	1.5895E−7
$\Delta t/\Delta t_l$	24.32	24.32	24.32	24.32	24.32

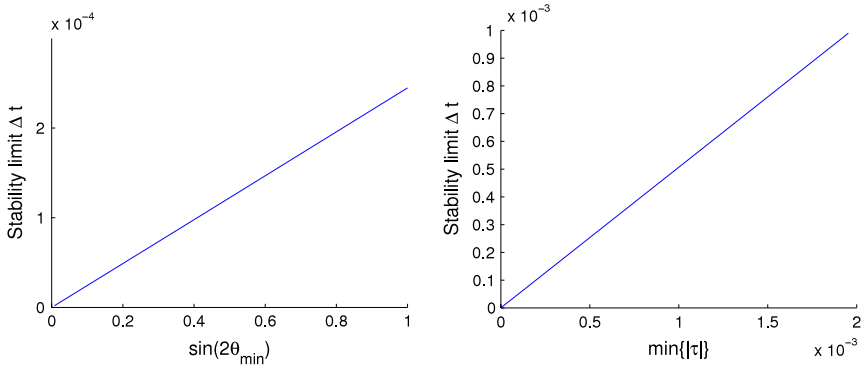


Fig. 3. Plots against $\sin(2\theta)$ of the stability limit Δt on a uniform shape irregular mesh (left); Plots against the smallest element area of the stability limit Δt on an adaptive non-uniform shape regular mesh (right).

5.2. The adaptive mesh cases

In the third example, we test one non-uniform mesh with regular shapes as shown in Fig. 2(a), which is very typical in adaptive finite element computation. In this triangulation, all elements are isosceles right triangles. We denote the level of refinement by $2k$, and then the edge length of the smallest element is $1/2^k$. In this case, $D_* = 8$, and $\mathcal{Q}_d(\tau) = 8$. Thus, by (32), for the linear element,

$$\Delta t_l < \frac{2}{8 \times 6} \times \frac{4 \min\limits_{\tau \in \mathcal{T}} |\tau|}{8} = \frac{\min\limits_{\tau \in \mathcal{T}} |\tau|}{48}. \tag{42}$$

The numerical stability limit Δt, the theoretical estimate Δt_l computed by (42), and the ratio $\Delta t/\Delta t_l$ are summarized in Table 3. We see that the ratio $\Delta t/\Delta t_l$ also approximates a constant, which shows that the analytic bound is sharp in terms of the geometric dependence. In order to demonstrate the relationship, in Fig. 3 (right), we plot with respect to the smallest element area, the curve of the stability limit Δt, which shows that the stability limit is proportional to the smallest element area in this case.

In the fourth example, a non-uniform mesh as shown in Fig. 2(b) with irregular shapes is used. In this triangulation, the elements on up-half domain are isosceles right triangles, while the elements on down-half domain are right triangles but with varying size and small angles $\theta_{\min}$. In this case, by (32),

$$\Delta t_l < \frac{2}{6 \times 6} \times \min_{\tau \in J} \left\{ \frac{S^{\tau}_{\min}}{Q_d(\tau)} \right\} = \frac{1}{18} \times \frac{6|\tau_{\min}|}{Q_d(\tau_{\min})} = \frac{1}{24} \times \frac{a^2 b^2}{a^2 + b^2},$$

where $a = 1/4$ is the length of long right edge of the smallest element, $b = 2^{-(k-2)}$ is the length of short right edge, k is the refinement level. The numerical results are presented in Table 4, from which we can see that the bound is sharp, up to only a constant algebraic factor, and the stable time step size is decided by the shortest edge length.

6. Conclusion and future work

In this paper, the relations between the stable time step size and mesh geometry for the explicit Euler-type time integration scheme coupled with a general finite element discretization defined on a simplicial mesh are explored systematically. The results are rigorously derived and are applicable to very general parabolic equations, finite element

Table 4
The stability limit on a non-uniform shape irregular mesh.

Mesh	4×8	4×10	4×12	4×14	4×16
Δt	1.9714E−4	1.2384E−5	7.7423E−7	4.8390E−8	3.0244E−9
Δt_l	1.0163E−5	6.3573E−7	3.9737E−8	2.4835E−9	1.5522E−10
$\Delta t/\Delta t_l$	19.40	19.48	19.48	19.48	19.48

spaces and geometric meshes. Better understanding of the effect of geometry on the stable time step size can lead to more efficient time marching. It is also useful for us to develop mesh generation and optimization strategies upon which a compromise between the efficiency of solver and the discretization error can be reached so that optimal performance of finite element computations can be achieved. There remain many issues to be explored in the future, for instance, the case without mass lumping [11], and the extensions to other interesting physical models. Some of these issues will be addressed in our future works.

Acknowledgments

The work of the first author is supported in part by the National Natural Science Foundation of China (No. 11001007), Research Fund for the Doctoral Program of Higher Education of China (No. 20101102120031) and the Fundamental Research Funds for the Central Universities (YWF-1002071). The work of the second author is supported in part by NSF DMS-1016073.

References

[1] Q. Du, Z. Huang, D. Wang, Mesh and Solver Coadaptation in finite element mehods for anisotropic problems, Numerical Methods for Partial Differential Equations 21 (2005) 859–874.
[2] Q. Du, D. Wang, L. Zhu, On mesh geometry and stiffness matrix conditioning for general finite element spaces, SIAM Journal on Numerical Analysis 47 (2009) 1421–1444.
[3] J. Shewchuk, What is a good linear finite element? Interpolation, conditioning, anisotropy and quality measures, Technical Report, CS, UC Berkeley, 2003.
[4] J.I. Lin, Bounds on eigenvalues of finite element systems, International Journal for Numerical Methods in Engineering 32 (1991) 957–967.
[5] I. Fried, Bounds on the spectral and maximum norms of the finite element stiffness, flexibility and mass matrices, International Journal of Solids and Structures 9 (1973) 1013–1034.
[6] I. Fried, Numerical Solution of Differential Equations, Academic Press, New York, 1979.
[7] J. Chen, S.C. Jardin, W. Park, J. Breslau, G. Fu, H.R. Strauss, L.E. Sugiyama, Application of mass lumped higher order finite elements in extended-MHD modeling, Princeton Plasma Physics Laboratory Report, 2005.
[8] M.J.S. Chin-Joe-Kong, W.A. Mulder, M. Van Veldhuizen, Higher-order triangular and tetrahedral finite elements with mass lumping for solving the wave equation, Journal of Engineering Mathematics 35 (1999) 405–426.
[9] S. Jund, S. Salmon, Arbitrary high-order finite element schemes and high-order mass lumping, International Journal of Applied Mathematics and Computer Science 17 (2007) 375–393.
[10] P. Ciarlet, Finite Element Method for Elliptic Problems, North-Holland, Amsterdam, 1978.
[11] L. Zhu, Q. Du, Mesh Dependent Stability and Condition Number Estimates for Finite Element Approximations of Parabolic Problems, 2010 (submitted for publication).